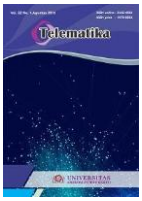

Available online at :
http://ejournal.amikompurwokerto.ac.id/index.php/telematika/

Telematika

Accreditated SINTA "2" Kemenristek/BRIN, No. 85/M/KPT/2020

Development of a Lightweight CNN Architecture for Multiclass Brain Tumor Detection Based on RGB Images

Ahmad Fauzi[1,*], Agus Heri Yunial[2]

[1,2] Department of Informatics Engineering, Faculty of Computer Science, Pamulang University, Tangerang selatan, Indonesia

ARTICLE INFO

History of the article:
Received August 15, 2025
Revised September 20, 2025
Accepted March 2, 2026

Keywords:

CNN
Brain Tumor Detection
Lightweight
Data Augmentation
Medical Image Classification

Correspondence:

E-mail:
dossen02621@unpam.ac.id

ABSTRACT

The identification of multiclass brain cancers from RGB MRI images presents a significant problem in medical diagnostics, necessitating high precision and computing efficiency. This research established a mid-lightweight Convolutional Neural Network (CNN) architecture utilizing Separable Convolution to identify three categories of brain tumors: glioma, meningioma, and pituitary. The model comprises five stratified SeparableConv2D blocks integrated with Batch Normalization, ReLU activation, and MaxPooling, succeeded by Global Average Pooling and three stratified dense layers (256, 128, 64 units) incorporating Dropout, culminating in a three-class softmax output layer. The total number of model parameters is 356,158 (1.36 MB), of which 354,174 are trainable, rendering it more efficient than traditional CNNs. Augmented data enhances generalization and mitigates overfitting. The model employs an Adam optimizer with a variable learning rate for training. The evaluation results indicated a training accuracy of 94.65%, a validation accuracy of 95.04%, an F1-score per class ranging from 0.95 to 0.96, and an AUC-ROC between 0.99 and 1.00, demonstrating consistent performance and exceptional discriminative capability. The study contribution involves the creation of a mid-lightweight CNN that is computationally efficient, sustains high accuracy in multiclass brain tumor classification, and utilizes minimal parameters. This paper addresses a deficiency in prior literature that frequently compromises accuracy in the development of lightweight CNN models for RGB imaging, while offering a robust architecture suitable for medical image-based auto-detection systems.

1. INTRODUCTION

The early identification of brain tumors is crucial in clinical practice as it directly influences treatment efficacy and patient survival rates. Imaging methods like Magnetic Resonance Imaging (MRI) offer a comprehensive structural depiction of brain tissue, facilitating the detection of gliomas, meningiomas, and pituitary tumors. (Akinyelu et al., 2022; Bhong, 2025; Hammad et al., 2023). Nonetheless, the manual interpretation of pictures by radiologists is constrained by prolonged analytic duration, inherent subjectivity, and the potential for human mistake, particularly in instances involving intricate tumor patterns.

The advancement of deep learning methodologies, especially Convolutional Neural Networks (CNN), has demonstrated a substantial enhancement in the classification of medical images (Feng, 2024; Kulkarni et al., 2024). CNN can autonomously and efficiently extract spatial features, yielding superior performance compared to traditional methods reliant on manually produced features (Batool & Byun, 2025; Leo et al., 2024). Contemporary designs, including ResNet, DenseNet, EfficientNet, and Vision Transformers, have been utilized in brain tumor diagnosis, demonstrating great accuracy on MRI datasets (Islam et al., 2024). Nevertheless, the majority of these models possess extensive parameters, varying from tens to hundreds of millions, necessitating substantial computational power and complicating deployment on low-resource devices. The Xception Architecture optimizes computational resource use and enhances predicted accuracy

by eliminating the need for preprocessing, segmentation, and augmentation approaches, resulting in a total of 20.88 million parameters for classification tasks (Korani et al., 2024).

The research gap originated from two primary sources. Primarily, the majority of light CNN research continues to utilize grayscale MRI imaging, although RGB pictures encompass differences in texture and color information that can enhance feature representation (Hammad et al., 2023). RGB-based methodologies are infrequently employed in mild CNN models, despite new research indicating that color can enhance the differentiation of tumor features more thoroughly. Secondly, despite numerous studies asserting that the model is "lightweight," the parameters employed remain rather substantial. For instance, MobileNet contains over 4 million parameters, EfficientNet-B0 comprises 5.3 million, but transfer-learning-based medical models typically exceed 20 million parameters (Batool & Byun, 2025; Islam et al., 2024; Rahman et al., 2023). This indicates that the genuinely lightweight solution (fewer than 500 thousand parameters) remains significantly constrained in the field of brain tumor detection.

Research literature indicates the urgency of automation and compares CNN performance, demonstrating its effectiveness in classifying brain cancers (Harahap et al., 2023; Khan et al., 2023; Krichen, 2023). This validates the advantages of automated solutions in alleviating the workload of radiologists (Bhong, 2025). Nevertheless, many studies fail to thoroughly examine the model's efficiency and continue to employ conventional structures that are very cumbersome. The study proposes the creation of a mid-lightweight CNN architecture utilizing Separable Convolution, comprising a total of 356,158 parameters, significantly fewer than other prevalent CNN models. The architecture comprises five multi-tiered convolutional blocks incorporating Batch Normalization, ReLU, and MaxPooling, succeeded by Global Average Pooling and three dense layers tailored for multiclass classification (glioma, meningioma, pituitary). This methodology aims to achieve a balance among precision, generalization ability, and computational efficiency.

The model was assessed using an MRI RGB dataset of three balanced classes, and scored based on accuracy, F1-score, and AUC-ROC. The experimental findings demonstrated exceptional performance, featuring a validation accuracy of 95.04% and an AUC-ROC ranging from 0.99 to 1.00, thereby confirming that the proposed architecture may deliver competitive results while utilizing a minimal amount of parameters. This study offers significant contributions, including the creation of a mid-lightweight CNN architecture with fewer than 400,000 parameters, the utilization of a lightweight model tailored for RGB-based MRI images, contrasting with prior research predominantly employing grayscale imagery, and the provision of an extensive evaluation employing clinical metrics alongside machine learning performance metrics. The suggested architecture is engineered for deployment on resource-constrained devices, facilitating the model's implementation in real-time clinical settings that demand computing economy while maintaining detection accuracy.

2. RESEARCH METHODS

2.1. Datasets and Data Characteristics

The research utilized the publicly accessible brain MRI dataset from the "Multi Cancer Dataset" in the Kaggle repository (Naren, 2022). The subset used for this investigation comprised 15,000 T1-weighted axial MRI scans, evenly distributed among three histologically verified categories: gliomas, meningiomas, and pituitary tumors, with 5,000 images allocated to each category. All photos possess three color channels with differing original resolutions, subsequently scaled to 224×224 pixels to conform to the proposed model's architecture. Figure 1 illustrates the characteristics of brain tumors in the brain cancer dataset.

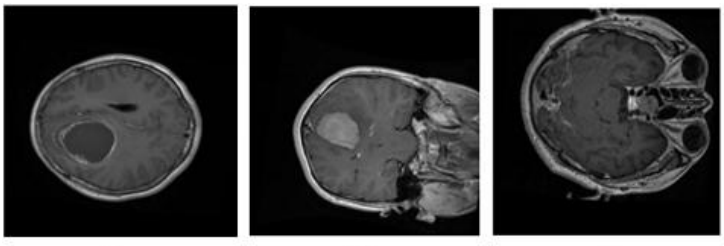

Figure 1. Characteristics Of Brain Tumors: (A) Glioma; (B) Meningioma; (C) Pituitary Tumor

The data was meticulously partitioned with a ratio of 0.8 for training and 0.2 for testing, while 0.2 of the training data was designated as a validation set by validation_split on the ImageDataGenerator (Akinyelu et al., 2022). This split guarantees that the model is assessed using data that has never been encountered during the training phase.

2.2. Preprocessing and Data Augmentation

All photos are normalized on a scale of 1/255, ensuring that the pixel values fall within the range of 0 to 1. The normalization procedure seeks to normalize the distribution of input values and expedite convergence during model training (Onakpojeruo et al., 2024). A real-time data augmentation technique was implemented utilizing ImageDataGenerator to enhance generalization capabilities and reduce the danger of overfitting (López-Sánchez et al., 2023). This augmentation encompasses geometric modifications, including rotation of up to 20°, horizontal and vertical shifts of 0.2, random zoom of 0.2, and shearing of 0.2. Furthermore, the image undergoes a horizontal flipping procedure and employs a closest fill mode to preserve pixel continuity across the extended region. The integration of these augmentation strategies systematically generates novel image variations that preserve the tumor's structural traits, enabling the model to learn feature representations more robustly and effectively in response to fluctuations in real-world image settings.

2.3. Proposed CNN Architecture

The CNN model presented in this paper employs a shallow-to-mid depth architecture designed to minimize the number of parameters and improve computational efficiency, while preserving the model's capacity to extract significant features from brain tumor images (Oluseyi et al., 2025). This architecture has many convolutional layers, succeeded by batch normalization, max pooling, and dropout layers to mitigate overfitting. The approach employs regularization techniques to enhance generalization and avert overfitting to the training data. Table 1: Architecture of the CNN Lightweight Model Utilizing Separable Convolution.

Table 1. CNN Architecture

Layer (Type)	Output Shape	Number of Parameters
SeparableConv2D	(224, 224, 32)	155
BatchNormalization	(224, 224, 32)	128
ReLU Activation	(224, 224, 32)	0
MaxPooling2D	(112, 112, 32)	0
SeparableConv2D	(112, 112, 64)	2,400
BatchNormalization	(112, 112, 64)	256
ReLU Activation	(112, 112, 64)	0
MaxPooling2D	(56, 56, 64)	0
SeparableConv2D	(56, 56, 128)	8,896
BatchNormalization	(56, 56, 128)	512
ReLU Activation	(56, 56, 128)	0
MaxPooling2D	(28, 28, 128)	0
SeparableConv2D	(28, 28, 256)	34,176
BatchNormalization	(28, 28, 256)	1,024
ReLU Activation	(28, 28, 256)	0
MaxPooling2D	(14, 14, 256)	0
SeparableConv2D	(14, 14, 512)	133,888
BatchNormalization	(14, 14, 512)	2,048
ReLU Activation	(14, 14, 512)	0
MaxPooling2D	(7, 7, 512)	0
GlobalAveragePooling2D	(512,)	0
Dense (256 units)	(256,)	131,328
Dropout (40%)	(256,)	0
Dense (128 units)	(128,)	32,896
Dropout (30%)	(128,)	0
Dense (64 units)	(64,)	8,256

Dropout (30%)	(64,)	0
Output Dense (Softmax, 3 classes)	(3,)	195

The suggested model is structured as a mid-lightweight Convolutional Neural Network utilizing separable convolution to optimize the performance-to-computational complexity ratio. The architecture executes feature extraction in stages via SeparableConv2D blocks, with the filter count escalating from 32 to 512. Each block incorporates Batch Normalization, ReLU activation, and MaxPooling to ensure gradient stability, expedite convergence, and diminish computational load. The distinction between depthwise and pointwise operations in separable convolution enhances discriminative capability while maintaining minimal parameter expansion. The spatial information were subsequently condensed using Global Average Pooling and then processed via three fully connected layers with 256, 128, and 64 neurons, incorporating Dropout as a regularization technique. This architecture, comprising 356,158 parameters (1.36 MB), provides enhanced memory and computational efficiency while ensuring training stability and generalizability on structurally complex brain MRI images, rendering it suitable for deployment on edge computing systems and resource-constrained devices.

2.4. Model Training Configuration

The model is developed using the TensorFlow Keras framework with an optimization approach designed to achieve optimal generalization. The weight updating process includes an Adam optimizer with an initial learning rate of 0.0005 and implements a Categorical Crossentropy function appropriate for multiclass categorization. The training was conducted for 50 epochs with a batch size of 32 to guarantee gradient stability and computational efficiency. To improve training quality and reduce overfitting, three callback mechanisms were utilized: EarlyStopping (patience = 5), ModelCheckpoint for optimal weight retention, and ReduceLROnPlateau for adaptive learning rate modification. The experiment was performed on the Kaggle platform using two T4 GPUs, Windows 11, Python 3.10, and TensorFlow 2.15, hence enabling an efficient and reproducible training process for the proposed mid-lightweight CNN architecture.

2.5. Model Evaluation

The model evaluation was conducted thoroughly using several performance indicators that reflected the quality of classification from both statistical and clinical viewpoints (Krichen, 2023). The study encompasses not only accuracy on training, validation, and testing datasets but also precision, recall, and F1-scores for each class, derived from the fundamental relationships inside the confusion matrix. Precision quantifies the accuracy of positive predictions and is defined as (Liu et al., 2024):

$$\text{Precision} = \frac{TP}{TP + FP} \tag{1}$$

Recall quantifies the ratio of true positive samples identified by the model, represented by the equation:

$$\text{Recall} = \frac{TP}{TP + FN} \tag{2}$$

The F1-score, representing the harmonic mean of precision and recall, is defined as:

$$\text{F1-Score} = 2 \cdot \frac{\text{Precision} \times \text{Recall}}{\text{Precision} + \text{Recall}} \tag{3}$$

Simultaneously, accuracy, utilized as a global performance metric for the model, is computed as the ratio of correct predictions to the total number of samples:

$$\text{Accuracy} = \frac{TP + TN}{TP + TN + FP + FN} \tag{4}$$

Moreover, the model's capacity to distinguish between classes was assessed using the Receiver Operating Characteristic–Area Under the Curve (ROC–AUC) for each class. The AUC value is defined as the integral of the curve representing the connection between the True Positive Rate (TPR) and the False Positive Rate (FPR).

$$\text{AUC} = \int_0^1 TPR(FPR)\, d(\text{FPR}) \tag{5}$$

The stability of the learning process was assessed by loss and accuracy curves over the epochs, indicating convergence, optimization dynamics, and the likelihood of overfitting or underfitting. This multifaceted evaluation method was selected to guarantee that the model exhibited not only superior predictive performance but also sufficient analytical reliability and robustness in clinical applications, where the precision of classification is essential for informed medical decision-making.

2.6. Research Workflow

This study's research flow is systematically arranged to offer a thorough overview of the steps of model creation, encompassing data collecting to final evaluation. The procedure commences with the acquisition of RGB-based MRI datasets, succeeded by preprocessing and augmentation phases to guarantee sufficient data quality and diversity. Moreover, the mid-lightweight CNN architecture is meticulously built and optimized prior to the training phase using the suitable hyperparameter setup. Upon completion of the model, a thorough evaluation is performed utilizing diverse performance criteria to measure accuracy, robustness, and generalizability. All stages are depicted in a flowchart to elucidate the interconnections among operations and guarantee the scientific reproducibility of the methodology. Figure 2 depicts the workflow and architecture of the Mid-Lightweight CNN.

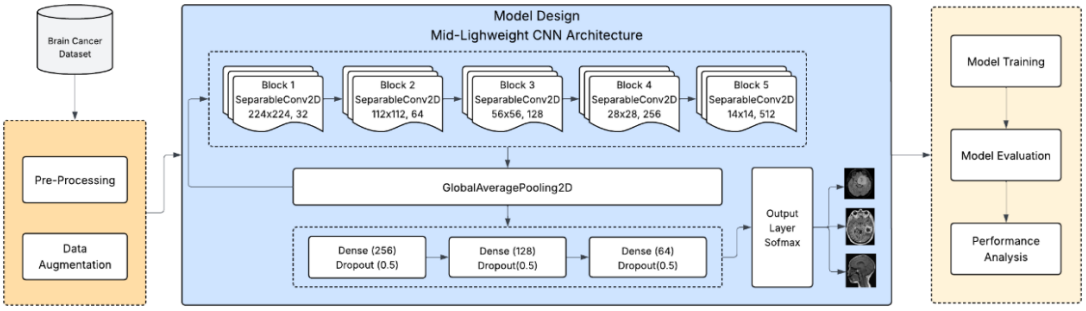

Figure 2. Workflow and Architecture Mid-Lightweight CNN

3. RESULTS AND DISCUSSION

This part methodically summarizes the experimental results, encompassing model architectural analysis, training performance, classification evaluation, and visual interpretation through loss accuracy graphs, confusion matrix, and ROC curves. All findings were assessed to verify performance consistency, generalization, and adherence to the stated lightweight claims.

3.1. Model Architecture

The created CNN model features a mid-lightweight architecture comprising a total of 356,158 parameters, of which 354,174 are trainable. The primary architecture comprises a tiered SeparableConv2D block for efficient feature extraction, succeeded by BatchNormalization to stabilize activation distribution, and MaxPooling to diminish spatial dimensions. The classification segment employs three densely connected layers (256, 128, 64) and dropout techniques for regularization. Figure 3 illustrates the architecture of the mid-lightweight CNN model.

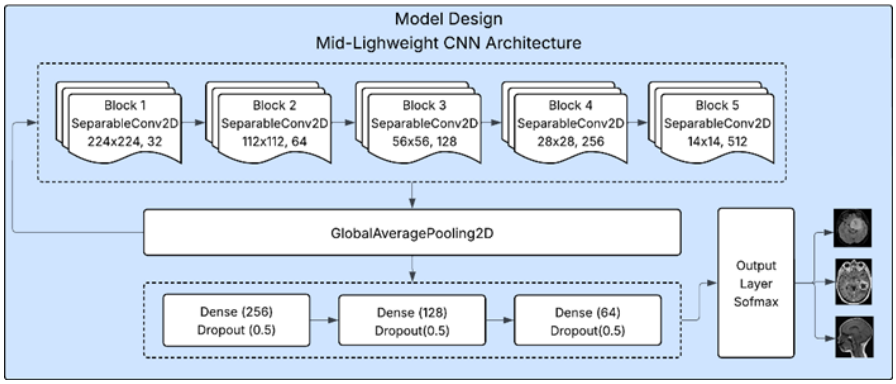

Figure 3. Architecture Mid-Lightweight CNN

3.2. Model Training Results

The training process demonstrated that the model had undergone a substantial enhancement in performance since the initial epoch. Despite the training being planned for 50 epochs, the model terminated at the 21st epoch due to the Early Stopping mechanism, indicating that convergence was reached more swiftly and that the proposed architecture demonstrated commendable computing efficiency. Table 2 summarizes the outcomes of the CNN model training.

Table 2. CNN Model Training Results

Epoch	Train Accuracy	Train Loss	Val Accuracy	Val Loss	LR
1	0.4934	1.4544	0.3333	1.5831	5e-04
5	0.8716	0.5213	0.6400	1.6869	5e-04
8	0.8995	0.3802	0.8421	0.5034	1.5e-04
11	0.9215	0.3191	0.9371	0.2556	1.5e-04
15	0.9393	0.2524	0.9529	0.2028	4.5e-05
18	0.9406	0.2493	0.9542	0.1992	4.5e-05
21 (End)	0.9496	0.2206	0.9504	0.2079	1.35e-05

The training results indicated that the CNN model exhibited a steady enhancement in performance with the progression of epochs. Initially, the training accuracy was suboptimal at 49.34%, accompanied by a validation accuracy of 33.33%, suggesting the model failed to discern critical patterns in the MRI imaging. During the mid-epoch (epochs 5–11), a notable enhancement was observed, with validation accuracy attaining 93.71% and validation loss diminishing to 0.2556. This pertains to the efficacy of optimization procedures, encompassing the application of SeparableConv2D and the learning rate scheduling mechanism. During the subsequent epoch, the model exhibited increased stability, achieving a peak validation accuracy of 95.42% in epoch 18. Notwithstanding minor variations in the concluding period, the overall performance sustained a high level, achieving a validation accuracy of 95.04% in the 21st epoch. The results indicate that the suggested architecture effectively generalizes to brain cancer MRI data, underscoring the importance of research aimed at enhancing classification accuracy via CNN-based model tuning.

Figure 4 illustrates a graph depicting accuracy and loss throughout the training process. The accuracy trend exhibited a constant rise from epoch 1 to 21, with a stable gap between training accuracy and validation accuracy, signifying that the model was not overfitting. The loss pattern diminished steadily and stabilized in the latter epochs, signifying that the model is attaining convergence effectively. The stability is enhanced by employing SeparableConv2D, BatchNormalization, and dropout, which contribute to preserving the model's generalization.

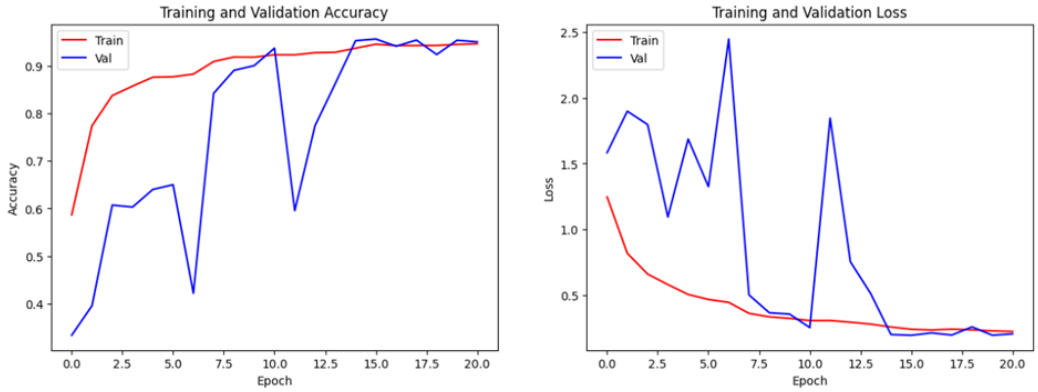

Figure 4. Graph illustrating Accuracy, Training Loss, and Validation Loss

3.3. Classification Evaluation on Test Data

The assessment was performed meticulously utilizing precision, recall, F1-score, and AUC–ROC metrics for each category. Table 3 presents the classification performance of the model across three kinds of brain tumors.

Table 3. Results of Evaluation of the Brain Tumor Classification Model

Class	Precision	Recall	F1-Score	AUC-ROC
Brain_Glioma	0.94	0.95	0.95	0.99
Brain_Meningioma	0.95	0.96	0.96	0.99
Brain_Tumor	0.96	0.94	0.95	1.00
Average (Macro)	0.95	0.95	0.95	0.996

The evaluation findings of the Brain Tumor Classification Model indicated that the model consistently achieved high performance in classification across all classes. The precision, recall, and F1-score values range from 0.94 to 0.96, indicating the model's proficiency in properly identifying positive samples and sustaining a consistent detection rate across all categories. The Brain_Glioma and Brain_Meningioma classes exhibited balanced performance with F1-scores of 0.95 and 0.96, respectively, however the Brain_Tumor class had exceptional prediction accuracy with an AUC-ROC of 1.00.

The elevated ROC–AUC value across all classes (≥ 0.99) substantiates that the model possesses exceptional discriminative capability in differentiating brain tumor classes. Moreover, the training accuracy (0.9465) and validation accuracy (0.9504) indicated that the model did not exhibit substantial overfitting symptoms. The results affirm that the employed classification method demonstrates dependable and consistent performance in identifying variations in brain tumor kinds within the utilized dataset.

The confusion matrix in figure 5 indicates that the model delivers highly consistent predictions across all three tumor classifications. The Brain Tumor class demonstrates an exceptionally high accuracy in prediction, reflected by a ROC score of 1.00. Notwithstanding certain classifications mistakes within the meningioma category, the model attained an F1-score of 0.96, signifying robust generalization skills to the test data.

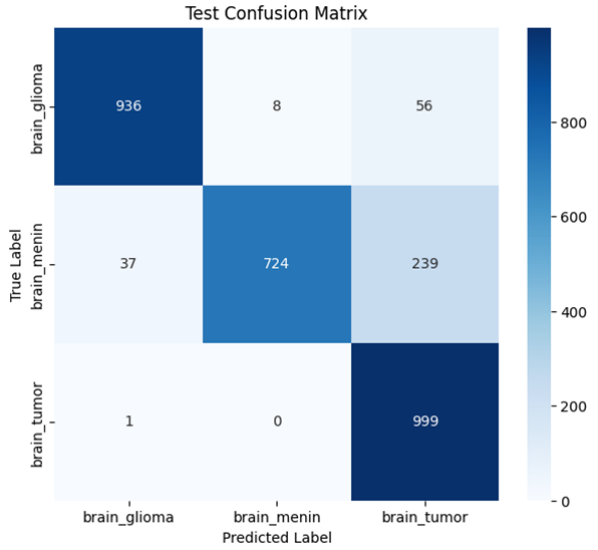

Figure 5. Confusion Matrix of Test Data

The ROC curve in figure 6 demonstrates that the overall class possesses an AUC value of > 0.99, signifying an exceptional capacity to differentiate tumor classes. The Brain Tumor class attained an impeccable AUC score of 1.00, indicating that the model demonstrated near-perfect sensitivity and specificity in identifying this class.

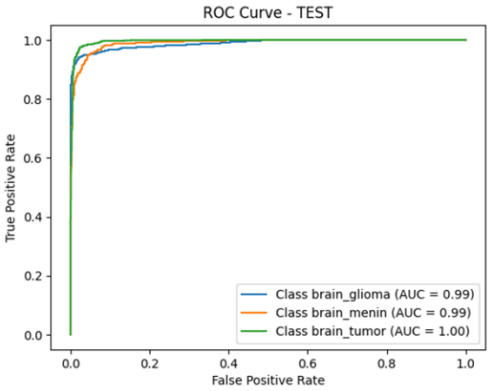

Figure 6. ROC-AUC Curve of Test Data

3.4. Discussion

This work illustrates that a mid-lightweight CNN design, with merely 356,158 parameters, may get classification performance on par with far bigger state-of-the-art models. This discovery aligns with recent research indicating that optimally designed lightweight systems can achieve high accuracy when complemented by robust regularization and data augmentation techniques (Hammad et al., 2023; Zhang et al., 2024).

(Zhang et al., 2024) attained 96% accuracy in thyroid cancer diagnosis employing a typical CNN with markedly greater model complexity, whilst (Li et al., 2025) showed 84% accuracy utilizing a conventional CNN. These findings suggest that performance is affected not only by model size, but also by architectural efficiency, regularization techniques, and augmentation methods. This work demonstrates that separable convolution improves adaptability to intricate texture fluctuations in RGB MRI pictures, which are fundamentally more difficult than grayscale medical imaging.

The proposed model demonstrates a significant efficiency advantage from a computational standpoint when compared to prevalent architectures such as EfficientNet-B0 (5.3 million parameters), EfficientNet-B3 (approximately 12 million), ResNet50 (25 million), and Xception (20.88 million) (Ali et al., 2025; Islam et al., 2024; Korani et al., 2024). The model, comprising roughly 356k parameters, is over 14 times lighter than EfficientNet-B0 and more than 30 times lighter than EfficientNet-B3, rendering it highly suitable for deployment in mobile, embedded, and edge-based healthcare systems.

(Batool & Byun, 2025) provide comparable evidence for lightweight design, achieving 96.03% accuracy with a multi-path lightweight CNN, while (Hossain et al., 2023) illustrate that lightweight Self-ONN architectures can diminish computational complexity by more than 70% while preserving competitive performance. Despite EfficientNet-B3 attaining a superior accuracy of 99.69% (Islam et al., 2024), this enhancement resulted in a substantial increase in model complexity.

This study demonstrates that an inherently lightweight architecture is a more practical and deployment-ready approach than post-hoc optimization of huge models, despite CNN pruning techniques being able to reduce model size with minimal accuracy loss (Sivakumar & Padmapriya, 2024). These results show that lightweight CNN architecture is not simply an optimization trend but an essential necessity for practical clinical applications. In accordance with current literature, the suggested mid-lightweight model attains an advantageous equilibrium among accuracy, stability, and computational efficiency, exhibiting strong generalization on intricate RGB MRI datasets and affirming its appropriateness for scaled medical imaging implementation.

3.5. Analysis of Overfitting and Generalization

This study rigorously assesses the model's stability using a blend of metrics and training curve visualization. The findings indicated that the model did not exhibit notable signs of overfitting. The minimal disparity between training accuracy at 0.9496 and validation accuracy at 0.9504 strongly indicates that the model does not only recall the training data, but rather learns consistent and representational patterns. Secondly, the training and validation loss curves exhibit no divergence; both decreased in tandem until converging at the 21st epoch, despite the training being planned for a total of 50 epochs. This fact demonstrates that regularization techniques, such as cascading dropouts and batch normalizing, efficiently preserve the stability of the activation distribution.

The elevated ROC–AUC scores for all three classes (0.99–1.00) indicate robust discriminative power in the new data, validating the model's applicability to previously unobserved data distributions. Data augmentation is crucial for enhancing model robustness by introducing visual variability through

rotation, shifting, zooming, and flipping, enabling the model to extract invariant properties without becoming fixated on the specific attributes of the training images. The integration of structural regularization, data augmentation, and learning rate adaptation effectively diminished prediction variance and prevented model overfitting, while ensuring that the performance achieved demonstrates exceptional generalization capability in the realm of MRI RGB-based brain tumor classification.

4. CONCLUSIONS AND RECOMMENDATIONS

The study's results consistently demonstrate that the mid-lightweight CNN architecture designed achieves great performance while preserving computational efficiency. This model, comprising merely 356,158 parameters, belongs to the lightweight architecture category yet remains competitive with larger models like ResNet50 and EfficientNet. The classification performance was outstanding, evidenced by a validation accuracy of 95.04%, a ROC–AUC value between 0.99 and 1.00, and precision, recall, and F1-score metrics ranging from 0.94 to 0.96 across all classifications of brain tumors.

The performance features are complemented by the model's robust stability, as evidenced by the training curve, which displays no signs of overfitting. The model's capacity to attain convergence by the 21st epoch out of a total of 50 epochs demonstrates exceptional learning efficiency. These findings affirm that architectural design methods, the implementation of separable convolution, batch normalization, and dropout techniques are crucial in sustaining a balance between model capacity and predictive efficacy.

The suggested model is a promising contender for implementation on low-resource devices, such as embedded systems and edge computing-based clinical applications, particularly in real-time medical diagnosis scenarios. This architecture's efficiency, high accuracy, stability, and generalizability constitute a substantial advancement in the creation of a CNN-based brain tumor classification system that is practical, lightweight, and suitable for real-world application.

This work illustrates that the suggested lightweight CNN model for brain tumor detection utilizing RGB images attains great accuracy (>95%) alongside exceptional computational efficiency. Notwithstanding the utilization of low-resolution images (224x224), the model proficiently identifies and categorizes multiclass brain cancers (glioma, meningioma, pituitary). Employing data augmentation and an adjusted learning rate during training enables the model to circumvent overfitting and achieve stable convergence more rapidly.

REFERENCES

Akinyelu, A. A., Zaccagna, F., Grist, J. T., Castelli, M., & Rundo, L. (2022). Brain Tumor Diagnosis Using Machine Learning, Convolutional Neural Networks, Capsule Neural Networks and Vision Transformers, Applied to MRI: A Survey. *Journal of Imaging*, *8*(8), 205. https://doi.org/10.3390/jimaging8080205

Ali, R. R., Yaacob, N. M., Alqaryouti, M. H., Sadeq, A. E., Doheir, M., Iqtait, M., Rachmawanto, E. H., Sari, C. A., & Yaacob, S. S. (2025). Learning Architecture for Brain Tumor Classification Based on Deep Convolutional Neural Network: Classic and ResNet50. *Diagnostics*, *15*(5), 624. https://doi.org/10.3390/diagnostics15050624

Batool, A., & Byun, Y. C. (2025). A lightweight multi-path convolutional neural network architecture using optimal features selection for multiclass classification of brain tumor using magnetic resonance images. *Results in Engineering*, *25*. https://doi.org/10.1016/j.rineng.2025.104327

Bhong, P. (2025). Brain Tumor Detection : CNN Based Brain Tumor Detection for MRI Scan. *Interantional Journal of Scientific Research in Engineering and Management*, *09*(05), 1–9. https://doi.org/10.55041/ijsrem47719

Feng, H. (2024). Brain Tumor Prediction and Analysis Based on Simple CNN. *Applied and Computational Engineering*, *38*(1), 267–273. https://doi.org/10.54254/2755-2721/38/20230562

Hammad, M., ElAffendi, M., Ateya, A. A., & Abd El-Latif, A. A. (2023). Efficient Brain Tumor Detection with Lightweight End-to-End Deep Learning Model. *Cancers*, *15*(10). https://doi.org/10.3390/cancers15102837

Harahap, F. A. A., Nafisa, A. N., Purba, E. N. D. B., & Putri, N. A. (2023). Implementasi Algoritma Convolutional Neural Network Arsitektur Model Mobilenetv2 Dalam Klasifikasi Penyakit Tumor Otak Glioma, Pituitary Dan Meningioma. *Jurnal Teknologi Informasi Komputer Dan Aplikasinya (Jtika)*, *5*(1), 53–61. https://doi.org/10.29303/jtika.v5i1.234

Hossain, A., Islam, M. T., Rahman, T., Chowdhury, M. E. H., Tahir, A., Kiranyaz, S., Mat, K., Beng, G. K., & Soliman, M. S. (2023). Brain Tumor Segmentation and Classification from Sensor-Based Portable Microwave Brain Imaging System Using Lightweight Deep Learning Models. *Biosensors*, *13*(3). https://doi.org/10.3390/bios13030302

Islam, M. M., Talukder, M. A., Uddin, M. A., Akhter, A., & Khalid, M. (2024). BrainNet: Precision Brain Tumor Classification with Optimized EfficientNet Architecture. *International Journal of Intelligent Systems*, *2024*. https://doi.org/10.1155/2024/3583612

Khan, S. S. A., Prova, A. A., & Acharjee, U. K. (2023). MRI-based Brain Tumor Image Classification Using CNN. *Asian Journal of Research in Computer Science*, 1–10. https://doi.org/10.9734/ajrcos/2023/v15i1310

Korani, W., Domakonda, S. S., & Kumar, P. M. (2024). Early Detection of Brain Tumor Using Mri and Transfer Learning. *Biomedical Engineering Applications Basis and Communications*, *37*(02). https://doi.org/10.4015/s1016237224300062

Krichen, M. (2023). Convolutional Neural Networks: A Survey. *Computers*, *12*(8), 151. https://doi.org/10.3390/computers12080151

Kulkarni, S., Bhosale, P., & Das, S. (2024). *Using CNN for Brain Tumor Diagnosis*. 104–124. https://doi.org/10.4018/979-8-3693-3629-8.ch006

Leo, H., Saddami, K., Roslidar, Muharar, R., Munadi, K., & Arnia, F. (2024). Lightweight Convolutional Neural Network (CNN) Model for Obesity Early Detection Using Thermal Images. *Digital Health*, *10*. https://doi.org/10.1177/20552076241271639

Li, Y., Li, T., He, K., Cui, X., Zhang, L., Wei, X., Liu, Z., & Wu, M. (2025). A Predictive Nomogram of Thyroid Nodules Based on Deep Learning Ultrasound Image Analysis. *Frontiers in Endocrinology*, *16*. https://doi.org/10.3389/fendo.2025.1504412

Liu, S., Yue, W., Guo, Z., & Wang, L. (2024). Multi-Branch CNN and Grouping Cascade Attention for Medical Image Classification. *Scientific Reports*, *14*(1). https://doi.org/10.1038/s41598-024-64982-w

López-Sánchez, M., Hernández-Ocaña, B., Chávez-Bosquez, O., & Hernández-Torruco, J. (2023). Supervised Deep Learning Techniques for Image Description: A Systematic Review. *Entropy*, *25*(4), 553. https://doi.org/10.3390/e25040553

Naren, O. S. (2022). *Multi Cancer Dataset*. Kaggle. https://doi.org/10.34740/KAGGLE/DSV/9537604

Oluseyi, O. M. O. O. M., Udofot, A. I. U. A. I., & Edim, E. B. E. E. B. (2025). Enhancing Medical Image Diagnosis Using Convolutional Neural Network and Transfer Learning. *Ijaem*, *7*(1), 131–139. https://doi.org/10.35629/5252-0701131139

Onakpojeruo, E. P., Mustapha, M. T., Ozsahin, D. U., & Özşahin, İ. (2024). Enhanced MRI-based Brain Tumour Classification With a Novel Pix2pix Generative Adversarial Network Augmentation Framework. *Brain Communications*, *6*(6). https://doi.org/10.1093/braincomms/fcae372

Rahman, H., Bukht, T. F. N., Ahmad, R., Almadhor, A., & Javed, A. R. (2023). Efficient Breast Cancer Diagnosis From Complex Mammographic Images Using Deep Convolutional Neural Network. *Computational Intelligence and Neuroscience*, *2023*(1). https://doi.org/10.1155/2023/7717712

Sivakumar, M., & Padmapriya, S. T. (2024). Improving Efficiency of Brain Tumor Classification Models Using Pruning Techniques. *Current Medical Imaging Formerly Current Medical Imaging Reviews*, *20*. https://doi.org/10.2174/0115734056303076240614113525

Zhang, X., Jia, C. C., Sun, M., & Ma, Z. (2024). The Application Value of Deep Learning-Based Nomograms in Benign–malignant Discrimination of TI-RADS Category 4 Thyroid Nodules. *Scientific Reports*, *14*(1). https://doi.org/10.1038/s41598-024-58668-6